How to cite: *Angew. Chem. Int. Ed.* **2021**, *60*, 15390–15398
International Edition: doi.org/10.1002/anie.202016757
German Edition: doi.org/10.1002/ange.202016757

DNA Structures | Hot Paper

Novel Insight into Proximal DNA Domain Interactions from Temperature-Controlled Electrospray Ionization Mass Spectrometry

*Adam Pruška, Adrien Marchand, and Renato Zenobi**

Abstract: *Quadruplexes are non-canonical nucleic acid structures essential for many cellular processes. Hybrid quadruplex–duplex oligonucleotide assemblies comprised of multiple domains are challenging to study with conventional biophysical methods due to their structural complexity. Here, we introduce a novel method based on native mass spectrometry (MS) coupled with a custom-built temperature-controlled nanoelectrospray ionization (TCnESI) source designed to investigate interactions between proximal DNA domains. Thermal denaturation experiments were aimed to study unfolding of multi-stranded oligonucleotide constructs derived from biologically relevant structures and to identify unfolding intermediates. Using the TCnESI MS, we observed changes in T_m and thermodynamic characteristics of proximal DNA domains depending on the number of domains, their position, and order in a single experiment.*

Introduction

The best-known oligonucleotide structure is the canonical double helix, but oligonucleotides can form many other secondary structures such as triplexes, guanine-quadruplexes, and *i*-motifs, by non-canonical base pair interactions. Guanine-quadruplexes, usually referred to as G-quadruplexes (GQs), are especially interesting secondary oligonucleotide structures because they play an important functional role in cellular processes, including DNA replication, transcription, translation, and telomere shortening.[1] GQ structures, which consist of a stack of G-quartets, are strongly favored in the presence of mono- and divalent cations (Figure 1), potassium being particularly suitable because it has the highest affinity for GQs.[2] G-quartets, four guanine bases arranged in a planar structure, are stabilized by Hoogsteen hydrogen-bonding interactions,[3] π-π stacking,[4] and hydrophobic interactions.[5] Factors that have a significant impact on GQ stability are the number of guanines involved,[6] the number of stacked G-quartets, loop length,[7,8] and the type of intercalated cations.[8]

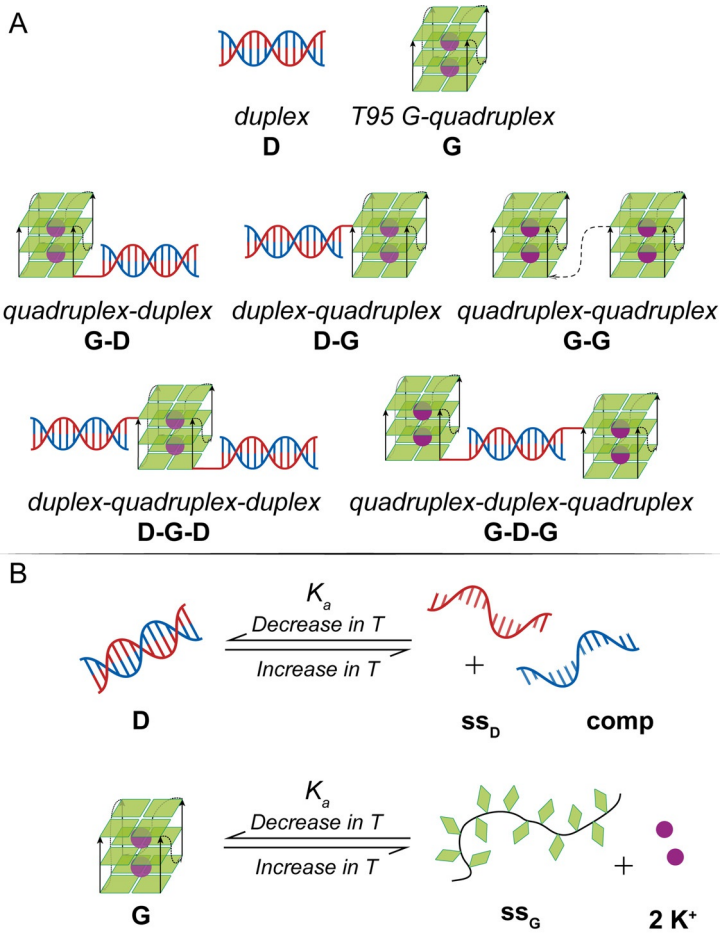

Figure 1. A) Overview of the structures and notations of the DNA complexes studied. B) Chemical equilibria of two single-domain DNA complexes showing unfolding of duplex (top) and model T95 G-quadruplex (bottom) upon increased temperature. Unfolding of individual domains causes a mass difference, which can be detected using mass spectrometry.

GQ structures are highly abundant in the genome and are typically localized in gene promoters, telomeres or minisatellites.[9] Functions of GQs have been extensively studied, primarily for their regulatory roles especially in gene expression and telomere shortening. Remarkably, GQs that are stable in vivo can both down- and up-regulate gene expression, depending on their location in the gene promoters.[10] GQ structures can, for example, act as physical obstacles to downregulate gene expression or block replication entirely.

Conversely, enhanced transcription could explain the upregulation effects, by favoring the binding of specific transcription factors to the folded GQ structures against

[*] A. Pruška, Dr. A. Marchand, Prof. Dr. R. Zenobi
Department of Chemistry and Applied Biosciences, ETH Zurich
Vladimir-Prelog-Weg 3, 8093 Zurich (Switzerland)
E-mail: zenobi@org.chem.ethz.ch
Supporting information and the ORCID identification number(s) for the author(s) of this article can be found under: https://doi.org/10.1002/anie.202016757.

random strands.[10,11] Additionally, putative GQ-forming regions have been located in the promoters of oncogenes, such as c-MYC, c-KIT, KRAS, BCL2, hTERT, and VEGFA[12–17] as well as at telomeres,[18] immunoglobulin switch regions,[19] and insulin regulatory regions.[20] In addition to eukaryotic cells, putative GQ-forming regions are present in the genomes of many viruses, including human immunodeficiency virus-1, Ebola virus disease, Zika virus, and SARS-COV-2 and many more.[21–28]

Besides understanding the natural function, GQs have been applied in nanodevices, aptamers, and for drug delivery.[29–31] Although GQ structures are self-assembling they usually exist as parts of single-stranded oligonucleotides with various proximal domains such as double helices (dsDNAs, duplexes), hairpins, *i*-motifs or additional GQs, which can have a significant impact on GQ functionality.[32–35] Much less is known about the folds of oligonucleotides in which multiple domains are formed from two or more nucleotide strands. The characterization of these structures and their functions is important for their biological roles and usage as aptamer-based drugs.[36]

G-quadruplexes are commonly studied using spectroscopic,[37–39] crystallographic,[40] computational,[41] biological,[42] and biophysical[43] techniques, to understand their structure,

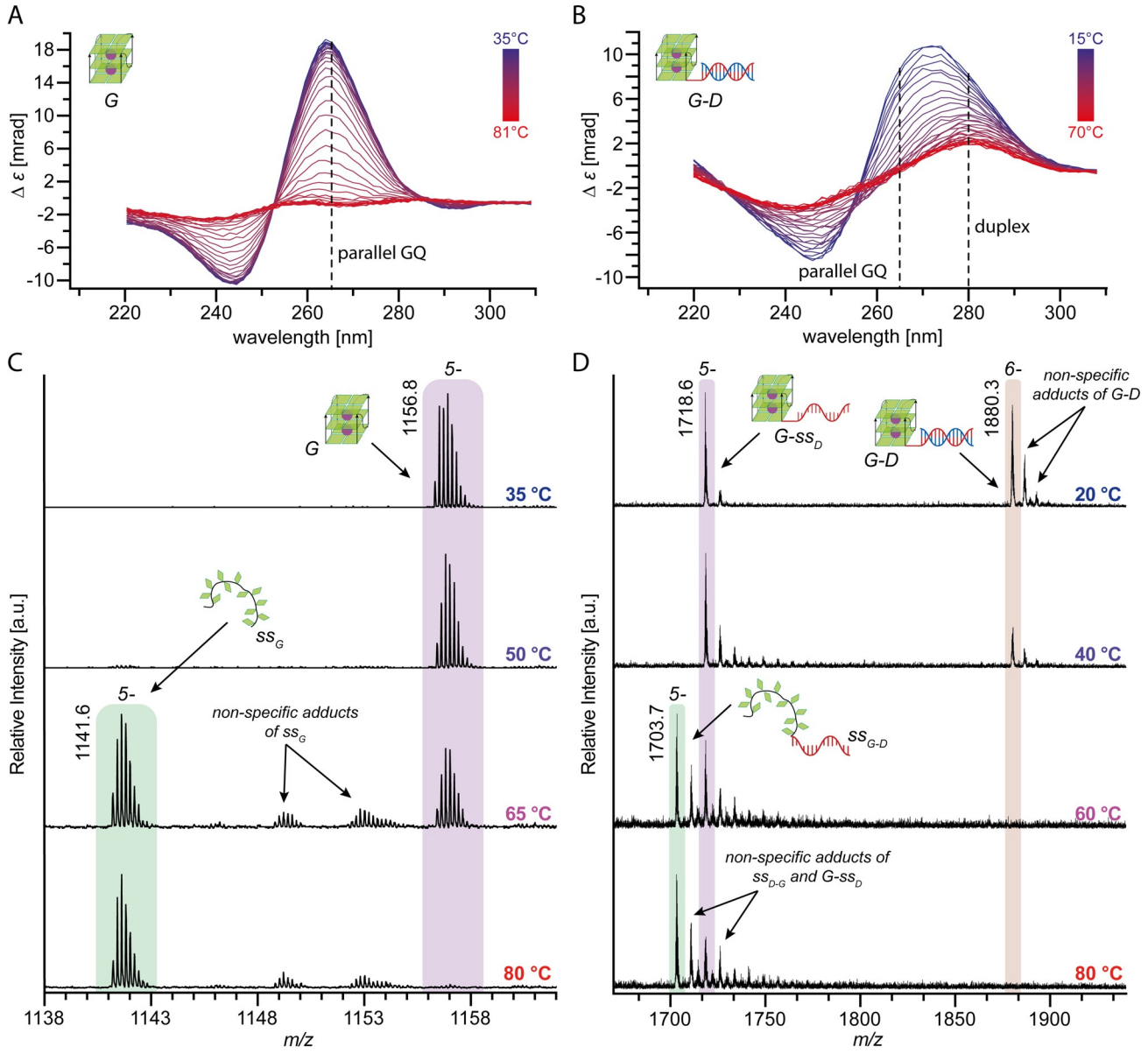

Figure 2. Comparison of CD and mass spectra of single-domain and two-domain DNA complexes at different temperatures. A) CD spectra of single T95 GQ and B) CD spectra of two-domain *G-D* complex showing spectral overlap of the individual domain CD profiles. Dashed lines highlight wavelengths chosen for CD melting (duplex, 280 nm; fully parallel GQ, 265 nm). Melting profiles are shown in Figure S1. C) Mass spectra of the T95 GQ at different temperatures showing specific signals of the DNA strand bound to 2 K^+, (folded GQ, *m/z* 1156.8) and the DNA strand without any K^+ (unfolded GQ, *m/z* 1141.6). D) Mass spectra of *G-D* complex at different temperatures. As labelled, the observed *m/z* signals correspond to the folded complex (*m/z* 1880.3), a semi-folded intermediate (*m/z* 1718.6), and the completely unfolded complex (*m/z* 1703.7). Average *m/z* values are shown. Full mass spectra showing charge state distributions can be found in Figure S9.

function, kinetics, and thermodynamics. Among other methods, circular dichroism (CD) and UV/Vis spectroscopy are well-established techniques to study structure and thermodynamics of oligonucleotide complexes. Both methods provide valuable information about GQs and do not require expensive apparatus and difficult sample preparation.[37,44–46]

DNA secondary structures can unfold upon temperature increase as sketched in Figure 1B. Each individual DNA domain is assigned a specific CD spectrum, which is used in conformational studies of DNA complexes and for the determination of the melting temperature (T_m). The T_m is a commonly used thermodynamic characteristic defined as the temperature at which 50% of a DNA complex is unfolded. An issue with much of the literature relying on CD spectroscopy is that T_m is usually defined only for a single, well-chosen wavelength, as indicated in Figures 2A and B.[37] For multi-domain complexes, the presence of more than one domain within the complex invariably results in spectral overlap. This complicates the choice of characteristic wavelengths for individual domains and thus precise determination of the T_m of each domain. However, mathematical analysis of CD spectra can be used to resolve the spectral contributions of individual domains in an chemical equilibrium.[47,48] Well known is a dual wavelength parametric test which can reveal complexity and underlying denaturation processes as demonstrated on GQs.[48] Furthermore, quantification of individual domains is particularly challenging using photometric spectroscopy.[49,50] In photometric melting experiments, one signal, usually representing a folded complex, is monitored and thus a two-state model must be assumed. Therefore, low-abundant and unstable intermediates remain a challenge to be identified and quantified when multi-domain complexes are investigated.

Native mass spectrometry (MS) is a technique in which intact non-covalent complexes are ionized from non-denaturing solvents.[51] "Native" conditions are usually seen as being as close as possible to physiological conditions, to prevent any changes during ion transport from ambient to the vacuum environment.[52–54] Electrospray ionization has significant limitations when analyzing solutions with salt concentration similar to cytosolic ones, but the ionic strength can be adjusted to similar levels using volatile salts.[55] Contrary to CD, mass spectrometry requires ionization and transfer of molecules into the gas phase where they are detected usually with an electron multiplier type detector. Our group recently demonstrated that native MS coupled with temperature-controlled nanoelectrospray (TCnESI) source is a useful analytical tools for structural biology and can retrieve detailed thermodynamic data on non-covalent complexes of peptides, proteins, and oligonucleotides.[56,57] MS can be beneficial in studies focusing on multi-domain oligonucleotide complexes where the number of potential intermediates is unknown or the intermediates occur at low abundance.

Table 1: DNA oligonucleotides used in the MS denaturation experiments.

Name (identifier)	Sequence (5′ to 3′)	Length [nt]	Average Mass [Da]
duplex-forming strand (ss_D)	d(CGCGAAGTA)	9	2747.86
comp. strand (ss_C)	d(TACTTCGCG)	9	2689.81
rev. duplex-forming strand (ss_D)	d(ATGAAGCGC)	9	2747.86
rev. comp. strand (ss_C)	d(GCGCTTCAT)	9	2689.81
T95 GQ (*G*)	$d(T(TGGG)_4T)$	18	5713.74
GQ-duplex (*G-D*)	$d(T(TGGG)_4TCGCGAAGTA)$	27	8523.56
duplex-GQ (*D-G*)	$d(ATGAAGCGCT(TGGG)_4T)$	27	8523.56
duplex-GQ-duplex (*D-G-D*)	$d(CGCGAAGTAT(TGGG)_4TCGCGAAGTA)$	36	11 333.39
GQ-GQ (*G-G*)	$d(T(TGGG)_4TT(TGGG)_4T)$	36	11 489.44
GQ-duplex-GQ (*G-D-G*)	$d(T(TGGG)_4TCGCGAAGTAT(TGGG)_4T)$	45	14 299.27

Here, we show that thermal denaturation coupled with native MS can be used to simultaneously detect individual forms of DNA multi-domain complexes over a large temperature range, from 15 to 90 °C. A set of DNA oligonucleotide multi-domain complexes were designed to represent various combinations of duplex and G-quadruplex domains (Figure 1A). If not specified otherwise, all samples were prepared in 100 mM trimethylammonium acetate (TMAA) to increase ionic strength and ionization efficiency. To identify the state of individual domains of multi-domain complexes, we use *D* for folded duplex, *G* for folded GQ, ss_D and ss_G for unfolded duplex-forming and GQ-forming sequences, respectively. Sequences and average masses are shown in Table 1.

Results and Discussion

We demonstrate that DNA multi-domain complexes can be characterized in detail and thermodynamic parameters can be obtained for each unfolding step individually using TCnESI mass spectrometry. To acquire melting temperatures and thermodynamic information the set of DNA complexes were electrosprayed while steadily increasing the temperature of the TCnESI source.

Determining the association constant (K_A) of each unfolding step with increasing temperature was possible by simultaneous detection of mass-to-charge ratios (m/z) that identify different complex forms. Upon unfolding of individual domains (Figure 1B), we detected a change of mass caused by loss of potassium cations or the complementary strand (for GQ or duplex, respectively). We then determine the thermodynamic parameters of individual unfolding steps using a van't Hoff analysis where the natural logarithm of K_A is plotted against the reciprocal value of absolute temperature ($1/T$). A detailed list of the associated equilibrium equations, and their respective Gibb's free energies ($\Delta G_A°$), enthalpies (ΔH_A), entropies (ΔS_A), and experimental T_m of all examined complexes associated with the folding of the particular complex domain is shown in Tables S1, S2 and is discussed in following sections.

Formation of the single T95-type GQ in 100 mM TMAA and 1 mM KCl can be readily proven using both CD spectroscopy (Figure 2A) and native MS (Figure 2C). On the contrary, a significant overlap occured in the CD spectra for the two-domain complex *G-D* consisting of both GQ and

duplex domains (Figure 2B). Upon melting experiments, we observed differences of several degrees in the T_m values for the single domains when comparing CD and native MS (Table S1). The different principles of the methods, the difference in required sample volumes, which in turn influences the heat capacity, and the duration of the analysis can all lead to differences in T_m. Regardless, the advantages of native MS make it an interesting alternative to established photometric methods. Hence, only the findings obtained using native MS are discussed in the following sections.

Duplex Domain Stability within Various Multi-Stranded Arrangements

Destabilization Effect of a G-Quadruplex

To study the effect of a proximal GQ on a duplex, we designed two sequences comprising a fully parallel T95 GQ forming sequence d(T(TGGG)$_4$T) placed on either the 5′ or 3′ end of a 9-base long duplex-forming region d(CGCGAAGTA). Single-stranded G-quadruplex-forming sequences (ss_G) form enthalpically favorable ($\Delta H_A < 0$) and entropically unfavorable ($\Delta S_A < 0$) GQ domains in 100 mM TMAA and 1 mM KCl solution. The GQ formation was spontaneous ($\Delta G_A° < 0$) at low temperatures for all investigated samples. The fully folded complex and an intermediate with an unfolded duplex of both *G-D* and *D-G* complexes were simultaneously identified in the mass spectra (using the difference in m/z) at the initial temperature of 20 °C (Figure 2D and S3, respectively).

In both cases, increasing the temperature initially led to unfolding of the duplex domain at ≈30 °C, followed by GQ unfolding at ≈60 °C (Figure 3A). The simultaneous detection of folded duplex and single strands allowed us to calculate the corresponding T_m. The T_m related to the duplex domain was significantly decreased, by 21 °C, compared to the self-contained duplex (Figure S1). A destabilizing effect was also observed when the GQ was attached to the 5′ end of the duplex (the MS thermal denaturation is shown in Figure S2). Additionally, we investigated two-domain complexes in the absence of K^+ to characterize the effects of an overhanging ss_G placed on the folded duplex ends. We observed a dominant signal of a folded duplex with an unfolded GQ domain (abbreviated as *D*-ss_G *or* ss_G-*D*) at the initial temperature of the MS thermal denaturation experiment, as shown in Figures S2A and S2B, respectively. A significant decrease in T_m of the duplex domain to 36.4 °C for *D*-ss_G and 35.9 °C for ss_G-*D*, respectively, was found, confirming the destabilizing effect of the flanking ss_G regions. The ss_G on the 3′ end was found to increase the $\Delta G_A°$ of the duplex to -32.2 ± 0.8 kJ mol^{-1}. When the ss_G was placed on the 5′ end of the duplex, we observed a comparable duplex destabilization (see Table S1). However, the presence of the folded GQ on either the 5′ or 3′ end of a duplex was found to destabilize the proximal duplex more compared to the ss_G flanking overhangs. A comparison of the striking destabilization effects of the GQ and ss_G domains on the proximal duplex is visualized in Figure 4A and shown in detail in Figure S4.

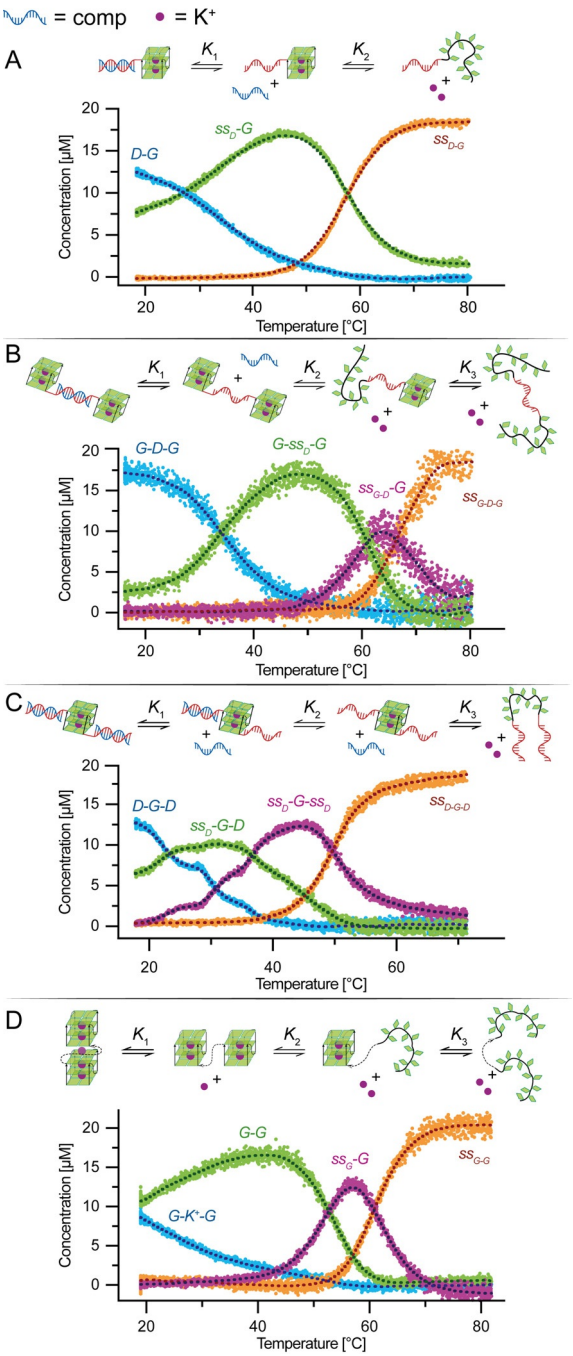

Figure 3. Thermal denaturation profiles acquired using TCnESI MS. Samples of 20 µM A) *D-G*, B) *G-D-G*, C) *D-G-D*, and D) *G-G* mixed with 20 µM complementary strand and 1 mM KCl were prepared in 100 mM TMAA. Three most abundant charge states were quantified using a 2.5 µM d(T)$_6$ solution as an internal standard and plotted as a function of time after the subtraction of the non-specific adduct contributions. Melting curves represent fully folded complex (●), first intermediate (●), second intermediate (●), and fully unfolded complex (●). The LOWESS method was used to generate regression curves. Cartoons of the corresponding chemical equilibria are depicted on the top, showing complex unfolding with identified intermediates.

As shown previously, we confirm that GQs have a destabilizing effect on proximal oligonucleotide domains.[50] Our

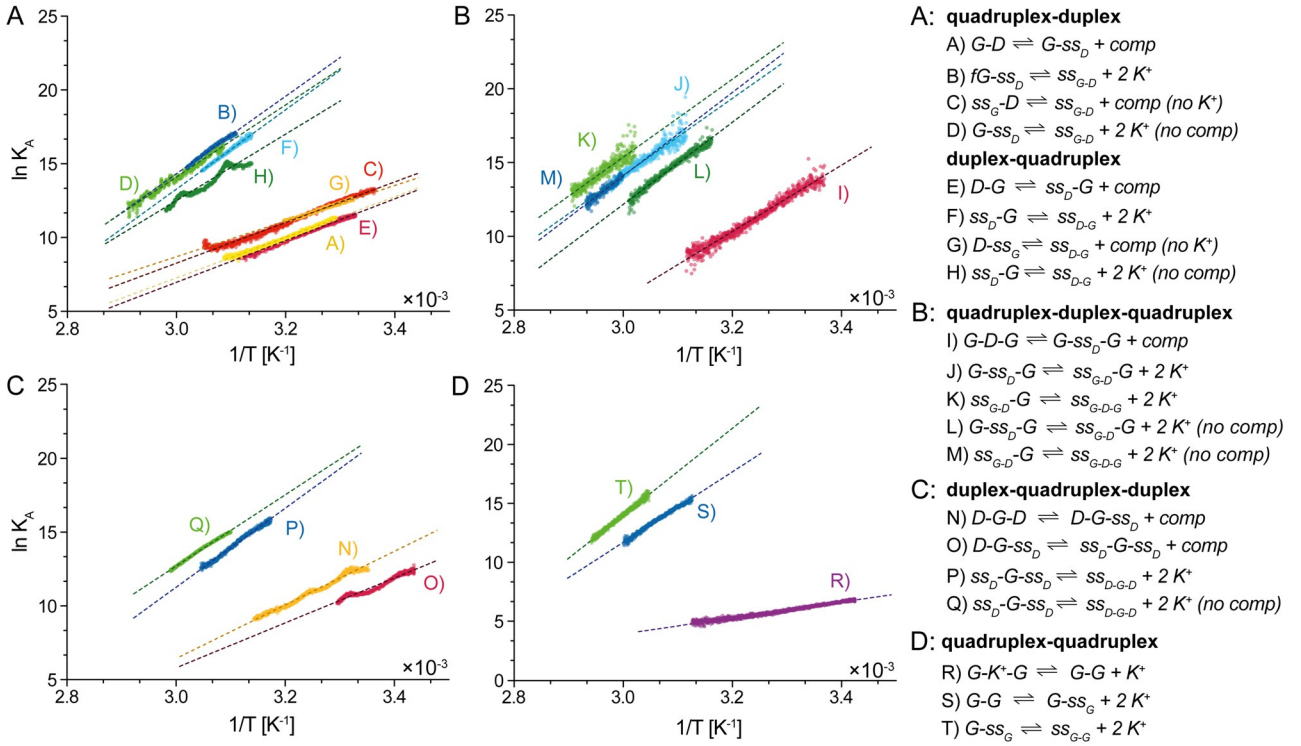

Figure 4. Van't Hoff analyses of the DNA domains stability contained in the investigated multi-domain complexes. Relevant equilibrium equations are listed on the right side. Regression curves associated with GQ domain folding are depicted in shades of green/blue and labeled with (B), (D), (F), (H), (J–M), (P–T) in the $1/T$ range of 2.85–3.15 K^{-1}. Unfolding of a higher-order GQ complex, (R), is depicted in purple and located in the duplex region suggesting low thermodynamic stability of this assembly. In the low temperature range ($1/T = 3.1$–3.45 K^{-1}), the regressions associated with duplex domains unfolding are labeled with (A), (C), (E), (G), (I), (N), and (O) are depicted in shades of yellow/red.

findings of the GQ's destabilizing effect are also supported by the work of Krauss et al., who investigated *D-G* junctions within monomolecular anti-thrombin aptamers.[36] Their findings suggested additional non-canonical interactions between the GQ loop and a proximal hairpin-loop-like duplex. A Wobble pairing between guanine and thymine or reverse Hoogsteen hydrogen bonds in the gradual transition between the duplex and GQ were detected using X-ray crystallography. Moreover, our findings are in agreement with a detailed NMR investigation of various types of unimolecular *D-G* systems carried out by Lim et al.[33] Generally speaking, their work documents the effects of GQ and duplex grooves, joining points, and loop lengths on the interaction between a duplex and GQ. Since the destabilization of the duplex is stronger in the presence of a folded GQ, the collected data point to the likelihood of specific interactions between the T95 GQ and the proximal duplex domain (Figure S5). However, compared to these previous studies, we focus on bimolecular complexes in which only one duplex strand was covalently linked to the GQ. Our results support the hypothesis that a single duplex could be destabilized by proximal domains, including overhanging strands and G-quadruplexes.

Synergic Effect of Two G-Quadruplexes

We further studied a complex with a T95 GQ on both ends of the duplex domain, which resulted in an even more significant duplex destabilization. Three solutions containing the d(T(TGGG)$_4$TCGCGAAGTAT(TGGG)$_4$T) oligonucleotide, a duplex complementary strand or potassium, or both, were investigated.

The most remarkable observation that emerged from this set of experiments was the establishment of a central duplex domain when both GQ domains were formed in presence of 1 mM KCl solution. The MS thermal denaturation experiment provided evidence for formed *G-D-G* in the low temperature range (Figure 3B). The duplex domain unfolded first, with a melting point of 34.3 ± 2.9 °C, followed by both GQs. Compared to the single duplex, the T_m of 34.3 °C is far below the original T_m of 50.7 °C for the simple duplex sequence (Table 1). When only one GQ was formed, the maximum abundance of the second intermediate was observed at 65 °C. We observed a significant re-stabilization of the central duplex when both GQs were formed. The $\Delta G_A°$ of this re-stabilized duplex domain within the *G-D-G* complex was -34.2 ± 1.8 kJ mol^{-1}, which is close to the $\Delta G_A°$ of the single duplex. The van't Hoff analysis of *G-ss$_D$-G* and *G-D-G* is shown in Figure 4B. In the absence of K^+, a destabilizing effect of two overhanging GQ-forming sequences resulted in a negligible abundance of the formed duplex domain under the chosen experimental conditions. We suggest an energetically unfavorable formation of the central duplex in the presence of two long overhanging GQ-forming sequences. A possible explanation could be related to steric effects of the overhangs. Above all, the results in this part show that the

duplex stability can be tuned by the presence of proximal GQ domains on both the 3′ and 5′ ends.

Stability of the GQ Affected by Various Multi-Domain Complex Arrangements

GQ structures were expected to affect the proximal duplex thermodynamics without being destabilized themselves. However, the interaction between various domains is mutual. We found that the position and primary structure of the overhanging strand have a significant role in the stability of the proximal GQ. To demonstrate this mutual effect, we performed a set of MS thermal denaturation experiments on multi-domain complexes containing GQs in various arrangements. When comparing the position of the overhang relative to GQ, we can see a difference in the stability of the GQ, which would be challenging to identify with conventional photometric methods.

Destabilization of the G-Quadruplex by an Adjacent Duplex

The T_m of the single GQ was 62.3 °C with $\Delta G_A°$ equal to $-60.5\ kJ\,mol^{-1}$. A significant destabilization occurred when the ss_D sequence was attached to the 5′ end compared to the 3′ end of the GQ. The ss_D-*G* showed a T_m decrease of ≈8.5 degrees to 53.7 ± 5.5 °C. When the duplex was formed (in the *D*-*G* complex), the destabilized GQ melted at $T_m = 57.8 \pm 2.4$ °C (Table S1). When the ss_D or duplex was placed on the 3′ end, the GQ stability was not significantly altered ($T_m =$ 62.2 ± 2.8 °C, 61.3 ± 3.2 °C, respectively) compared to individual T95 GQ. This suggests a stronger destabilization effect of overhanging strands compare to duplexes on the GQ. Moreover, the position of either ss_D or *D* plays a role in GQ destabilization, as demonstrated above. A detailed comparison of thermodynamic parameters can be found in Figure S6.

G-Quadruplex within Three-Domain Complexes

Furthermore, a GQ within higher-order three-domain complexes was investigated. We suspect that two duplex domains placed on both the 3′ and 5′ ends of the GQ structure might cause further destabilization of the central GQ. For this purpose, the sequence d(CGCGAAGTAT-$(TGGG)_4$TCGCGAAGTA), which forms one GQ between two duplexes, was chosen as a model system (see Figure 3C).

When the complementary strand, together with 1 mM K^+, was added to the mixture, both duplex domains and the central GQ were formed. Using the mass shift in the spectra, we identified the consequent unfolding of duplexes, followed by unfolding of the GQ. The T_m of the central GQ dropped to 49.8 ± 2.3 °C. The MS thermal denaturation of the fully formed *D*-*G*-*D* complex, which documents the presence of two intermediates, is depicted in Figure 3C. When MS thermal denaturation was performed in the absence of a complementary strand, unfolding of ss_D-*G*-ss_D was observed at higher temperature, $T_m = 54.9 \pm 1.5$ °C, compared to the GQ domain within *D*-*G*-*D* (Figure S2E). The van't Hoff analysis confirmed a synergistic destabilization effect of the two ss_D or formed duplexes placed on the 3′ and 5′ ends of the T95 GQ (see Figure 4C).

To test the destabilization of the GQ within another three-domain system, we tested the complex *G*-*D*-*G* in the presence of duplex complementary strand and 1 mM KCl. We observed the formation of the duplex domain between two folded GQs at room temperature. Subsequent unfolding of the duplex and GQ domains was observed, as demonstrated in Figure 3B. Absence of the duplex complementary strand resulted in formation of the complex *G*-ss_D-*G*. The MS thermal denaturation revealed the presence of one intermediate at ≈58 °C (Figure S2F). Based on the mass difference, we associated this intermediate with a complex containing only one formed GQ. Interestingly, Van't Hoff analysis in Figure 4B revealed that the formation of the central duplex restabilized both GQs and increased their T_m by 5–7 °C. However, the Gibbs free energy diagram of the *G*-*D*-*G* complex shows negligible energetic differences between individual domains and domains in *G*-*D*-*G* complex (Figure S5).

We identified a general trend of duplex destabilizing effect on the GQ depending on its position. A slightly higher destabilization of the T95 GQ occurs when the ss_D or duplex is placed on the 5′ end compared to the 3′ end. Moreover, it is evident that significantly higher GQ destabilization is observed in the presence of the formed duplex domains on both ends of the GQ. How the GQ stability is affected by a proximal overhanging strand or a formed duplex across various investigated systems is compared in Figure S6, which summarizes and compares thermodynamic parameters extracted from the van't Hoff analyses including calculated Gibbs free energies.

Stacking of Two G-Quadruplexes

Apart from the tested *G*-*D*-*G*, *c*omplexes containing two GQs with the sequence $d(GGGT)_4$ are generally prone to form higher-order multimeric assemblies. Many types of dimers have been described, including interlocked, bimolecular, homo, and hetero types.[58–60] To the best of our knowledge, this is the first time that a thermodynamic examination is performed on a monomolecular, two-domain homodimer. The sequence d(T$(TGGG)_4$TT$(TGGG)_4$T) will be abbreviated here as *G*-*G* complex. In contrast to previous MS experiments involving the GQ domain, we observed a mass difference of one potassium in the low temperature range between 20 and 40 °C (Figure 3D) at 1 mM KCl and 100 mM TMAA concentration. Based on the mass differences identified in the mass spectra, we suggest incorporation of one additional potassium cation (39 Da) between the two T95 GQs. This assembly can probably be assigned to a higher-order GQ with six planes of G-quartets stacked on top of each other (*G*-K^+-*G*), as shown in Figure 3D. Upon further increase of the temperature up to 85 °C, we identified two subsequent mass shifts (2 × 39 Da each) of two simultaneously released potassium cations, which documents the sequential unfolding of two individual GQs. The maximum abundance of the intermediate, which represents the form with only one folded GQ, occurred at 58 °C; above 70 °C, the completely unfolded form without any specifically bound potassium was

dominant. The results of the van't Hoff analysis (Figure 4D) further indicated a remarkable difference in the stability between the higher-order GQ and two individual GQ domains. Compared to the $\Delta G_A°$ of a single T95 GQ ($-60.5\ kJ\,mol^{-1}$), we observed destabilization of one GQ domain together with a stabilizing effect on the second GQ within the two-domain complex form. The Gibbs free energies were found to be -55.4 ± 1.8 and $-67.2 \pm 2.6\ kJ\,mol^{-1}$. Using the concept of thermodynamic linkage and coupling of free energies,[61] we highlighted the effect of formation of the higher-order GQ structure in Figure 5. CD analysis of *G-G* suggested the formation of an entirely parallel complex due to the presence of a specific absorption peak at 265 nm (Figure S7).

The corresponding mass spectra at various temperatures are shown in Figure S8. These findings support the work of Petraccone et al.[62] and confirm an energetically favorable stacking of two GQs on top of each other, creating one large, however, weak and at high temperature unstable complex with $\Delta G_A°$ of $-32.8 \pm 0.4\ kJ\,mol^{-1}$.

Furthermore, based on the significant difference of more than $17\ kJ\,mol^{-1}$ between individual GQs and *G-K⁺-G* complex, there is a tendency towards a new level of complexity associated with multiple GQ formation within one oligonucleotide, possibly affecting the interaction with specific ligands or GQ-binding proteins. Interestingly, the average of $\Delta G_A°$ values of both GQs is $-61.3\ kJ\,mol^{-1}$, which is negligibly different from the stability of the single T95 GQ (see Tables S1 and S2). This fact demonstrates the importance of identifying intermediates, which provides more detailed insight when characterizing the folding of GQs.

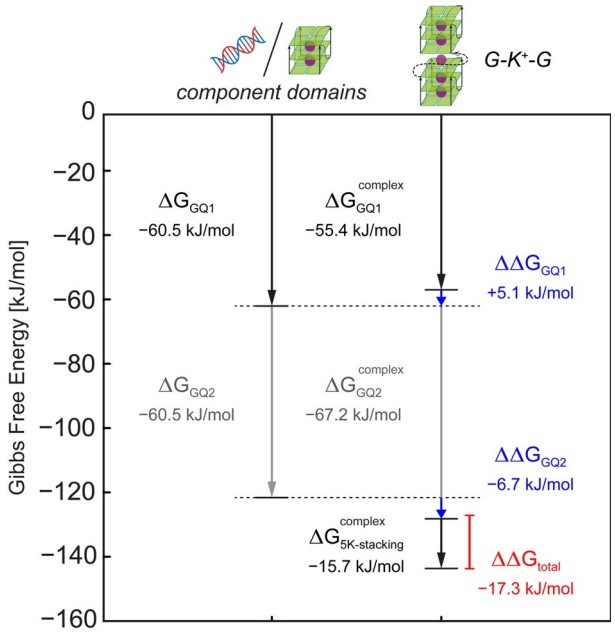

Figure 5. Energy diagram of coupling Gibbs free energy $\Delta\Delta G$ comparing the stability of the *G-K⁺-G* DNA complex and the sum of stabilities of individual domains. Differences between individual domains are shown in blue, showing destabilization of the GQ1 by $5.1\ kJ\,mol^{-1}$ and stabilization of the GQ2 by $-6.7\ kJ\,mol^{-1}$. The overall energy difference with a significant contribution of 5K-stacking is shown in red.

The *G-G* can be considered as the simplest model of a telomeric region, which is usually subject to multimerization between several GQs, although the sequence of telomeric regions usually contains a d(TTAGGG) motif, often with Sr^{2+} incorporated.[63,64] Previous studies have shown that a series of GQs in the telomere region can exist in the "beads-on-a-string" model[65] or be subject to loop-mediated stacking.[66,67] Our results go beyond these previous reports, showing that both structures can exist and their formation depends on the composition and length of the connecting string, as documented by the behavior of the *G-D-G* and *G-G* complexes. The mutual destabilization could be particularly important in processes involving GQ-specific helicases despite the suspected lower propensity of GQ to destabilization.

Conclusion

We have investigated the thermodynamic properties of multi-domain DNA complexes using native mass spectrometry coupled with a temperature-controlled nanoelectrospray (TCnESI) source. We validated the qualities of our method and demonstrated its potential and possibilities when applied to complex oligonucleotide systems with more than one domain. The enthalpic and entropic contributions could be directly determined for each domain individually using TCnESI MS. Our findings indicate a significant destabilizing effect of the T95 GQ on the duplex domain placed on either the 3′ or 5′ end. Remarkably, two fully folded GQs on both ends re-stabilized the central duplex domain. A significant difference in $\Delta G_A°$ revealed that the formation of GQ led to more substantial duplex destabilization compared to ss_G overhanging strands. We suggest that GQ stability can be affected by overhanging strands or duplexes even though the destabilization of T95 GQ located in some complexes was insignificant. Using Gibbs free energy diagrams, we can conclude that the order of domains and their primary structure is essential for the individual domain stability. Changing the order, as well as the primary structure, can regulate the thermodynamic stability of the DNA domains. Remarkably, the MS thermal denaturation provided direct evidence for stacking of GQ domains within a single-stranded *G-G* complex.

The most significant limitation of our method is the absence of information on the topology and domain orientation. The necessity of using volatile salts in the mM range in native MS could potentially lead to topological differences compared to the cellular environment. Moreover, the DNA base residues that are essential for domain interaction cannot be determined directly. Many oligonucleotide secondary structures, such as *i*-motifs, also do not show a mass difference when undergoing conformational changes. To address the latter challenge, we plan to implement ion-mobility spectrometry, which is capable of separation based on collision cross-section of identical m/z signals. Ion mobility-mass spectrometry also opens up an exciting possibility for this analytical technique, which would bring further insights into the thermodynamic characterization of more oligonucleotide complexes.

Overall, native MS, together with TCnESI, is a powerful method that supports established methods and can extend our knowledge about oligonucleotide complexes. Investigation of multi-domain DNA or RNA structures using our equipment and methodology together with established spectroscopic methods (UV/Vis, CD, NMR, and more) could bring more comprehensive thermodynamic information about the driving forces of folding processes. Mutual domain interactions can now be studied and described in a unique way. Our methodology could be particularly useful in studies of protein interactions with oligonucleotide structures, drug design, aptamer characterization, and biosensing.

Acknowledgements

Circular dichroism data were collected with the help of V. Islami from the Wennemers group at ETH Zurich. J. Rössinger is acknowledged for her contribution to the early stage of the project. We thank all members of the Zenobi group, particularly M. Köhler, J. Hajduk, I. Oganesyan, A. Begley, G. L. Bartolomeo, P. Bittner, and also B. Pavlatovská, A. Holfeld, V. Vojtěch for helpful discussion, suggestions, moral support, and asset. We thank the Swiss National Science Foundation for financial support of this work (grant number 200020_178765). The original data used in this publication are made available in a curated data archive at ETH Zurich (https://www.research-collection.ethz.ch) under the DOI https://doi.org/10.3929/ethz-b-000484315.

Conflict of interest

The authors declare no conflict of interest.

Keywords: G-quadruplexes · native mass spectrometry · oligonucleotides · temperature-controlled mass spectrometry · thermodynamics

[1] D. Rhodes, H. J. Lipps, *Nucleic Acids Res.* **2015**, *43*, 8627 – 8637.
[2] D. Bhattacharyya, G. M. Arachchilage, S. Basu, *Front. Chem.* **2016**, *4*, 38.
[3] K. Hoogsteen, *Acta Cryst.* **1963**, *16*, 907 – 916.
[4] G. W. Collie, S. M. Haider, S. Neidle, G. N. Parkinson, *Nucleic Acids Res.* **2010**, *38*, 5569 – 5580.
[5] C. J. Lech, B. Heddi, A. T. Phan, *Nucleic Acids Res.* **2013**, *41*, 2034 – 2046.
[6] X. M. Li, K. W. Zheng, J. Y. Zhang, H. H. Liu, Y. De He, B. F. Yuan, Y. H. Hao, Z. Tan, *Proc. Natl. Acad. Sci. USA* **2015**, *112*, 14581 – 14586.
[7] A. Guédin, J. Gros, P. Alberti, J. L. Mergny, *Nucleic Acids Res.* **2010**, *38*, 7858 – 7868.
[8] A. Risitano, K. R. Fox, *Org. Biomol. Chem.* **2003**, *1*, 1852 – 1855.
[9] S. Amrane, M. Adrian, B. Heddi, A. Serero, A. Nicolas, J. L. Mergny, A. T. Phan, *J. Am. Chem. Soc.* **2012**, *134*, 5807 – 5816.
[10] I. T. Holder, J. S. Hartig, *Chem. Biol.* **2014**, *21*, 1511 – 1521.
[11] J. Eddy, N. Maizels, *Nucleic Acids Res.* **2008**, *36*, 1321 – 1333.
[12] J. Seenisamy, E. M. Rezler, T. J. Powell, D. Tye, V. Gokhale, C. S. Joshi, A. Siddiqui-Jain, L. H. Hurley, *J. Am. Chem. Soc.* **2004**, *126*, 8702 – 8709.
[13] S. Rankin, A. P. Reszka, J. Huppert, M. Zloh, G. N. Parkinson, A. K. Todd, S. Ladame, S. Balasubramanian, S. Neidle, *J. Am. Chem. Soc.* **2005**, *127*, 10584 – 10589.
[14] S. Cogoi, L. E. Xodo, *Nucleic Acids Res.* **2006**, *34*, 2536 – 2549.
[15] J. Dai, T. S. Dexheimer, D. Chen, M. Carver, A. Ambrus, R. A. Jones, D. Yang, *J. Am. Chem. Soc.* **2006**, *128*, 1096 – 1098.
[16] S. L. Palumbo, S. W. Ebbinghaus, L. H. Hurley, *J. Am. Chem. Soc.* **2009**, *131*, 10878 – 10891.
[17] D. Sun, K. Guo, J. J. Rusche, L. H. Hurley, *Nucleic Acids Res.* **2005**, *33*, 6070 – 6080.
[18] E. H. Blackburn, *Nature* **1991**, *350*, 569 – 573.
[19] D. Sen, W. Gilbert, *Nature* **1988**, *334*, 364 – 366.
[20] M. C. U. Hammond-Kosack, M. W. Kilpatrick, K. Docherty, *J. Mol. Endocrinol.* **1993**, *10*, 121 – 126.
[21] P. Murat, J. Zhong, L. Lekieffre, N. P. Cowieson, J. L. Clancy, T. Preiss, S. Balasubramanian, R. Khanna, J. Tellam, *Nat. Chem. Biol.* **2014**, *10*, 358 – 364.
[22] S. Artusi, M. Nadai, R. Perrone, M. A. Biasolo, G. Palù, L. Flamand, A. Calistri, S. N. Richter, *Antiviral Res.* **2015**, *118*, 123 – 131.
[23] R. Perrone, M. Nadai, J. A. Poe, I. Frasson, M. Palumbo, G. Palù, T. E. Smithgall, S. N. Richter, *PLoS One* **2013**, *8*, e73121.
[24] B. Biswas, M. Kandpal, P. Vivekanandan, *Nucleic Acids Res.* **2017**, *45*, 11268 – 11280.
[25] S.-R. Wang, Y.-Q. Min, J.-Q. Wang, C.-X. Liu, B.-S. Fu, F. Wu, L.-Y. Wu, Z.-X. Qiao, Y.-Y. Song, G.-H. Xu, et al., *Sci. Adv.* **2016**, *2*, e1501535.
[26] S. R. Wang, Q. Y. Zhang, J. Q. Wang, X. Y. Ge, Y. Y. Song, Y. F. Wang, X. D. Li, B. S. Fu, G. H. Xu, B. Shu, et al., *Cell Chem. Biol.* **2016**, *23*, 1113 – 1122.
[27] A. M. Fleming, Y. Ding, A. Alenko, C. J. Burrows, *ACS Infect. Dis.* **2016**, *2*, 674 – 681.
[28] N. Panera, A. E. Tozzi, A. Alisi, *Drugs* **2020**, *80*, 941 – 946.
[29] H. Yaku, T. Murashima, D. Miyoshi, N. Sugimoto, *Sensors* **2015**, *15*, 9388 – 9403.
[30] C. Roxo, W. Kotkowiak, A. Pasternak, *Molecules* **2019**, *24*, 3781.
[31] Y. Yu, Y. Zhou, M. Zhu, G. Su, H. Deng, W. Chen, H. Peng, *Chem. Commun.* **2019**, *55*, 389 – 392.
[32] J. Ren, X. Qu, J. O. Trent, J. B. Chaires, *Nucleic Acids Res.* **2002**, *30*, 2307 – 2315.
[33] K. W. Lim, A. T. Phan, *Angew. Chem. Int. Ed.* **2013**, *52*, 8566 – 8569; *Angew. Chem.* **2013**, *125*, 8728 – 8731.
[34] K. W. Lim, Z. J. Khong, A. T. Phan, *Biochemistry* **2014**, *53*, 247 – 257.
[35] J. Zhou, S. Amrane, D. N. Korkut, A. Bourdoncle, H.-Z. He, D.-L. Ma, J.-L. Mergny, *Angew. Chem. Int. Ed.* **2013**, *52*, 7742 – 7746; *Angew. Chem.* **2013**, *125*, 7896 – 7900.
[36] I. Russo Krauss, V. Spiridonova, A. Pica, V. Napolitano, F. Sica, *Nucleic Acids Res.* **2016**, *44*, 983 – 991.
[37] J. L. Mergny, L. Lacroix, *Curr. Protoc. Nucleic Acid Chem.* **2009**, *37*, 17.1.1 – 17.1.15.
[38] R. del Villar-Guerra, J. O. Trent, J. B. Chaires, *Angew. Chem. Int. Ed.* **2018**, *57*, 7171 – 7175; *Angew. Chem.* **2018**, *130*, 7289 – 7293.
[39] M. Adrian, B. Heddi, A. T. Phan, *Methods* **2012**, *57*, 11 – 24.
[40] N. Campbell, G. W. Collie, S. Neidle, *Curr. Protoc. Nucleic Acid Chem.* **2012**, *50*, 17.6.1 – 17.6.22.
[41] S. Haider, *J. Indian Inst. Sci.* **2018**, *98*, 325 – 339.
[42] F. Raguseo, S. Chowdhury, A. Minard, M. Di Antonio, *Chem. Commun.* **2020**, *56*, 1317 – 1324.
[43] J. H. Bae, J. Z. Fang, D. Y. Zhang, *Nucleic Acids Res.* **2020**, *48*, e89.
[44] F. Rosu, V. Gabelica, C. Houssier, P. Colson, E. De Pauw, *Rapid Commun. Mass Spectrom.* **2002**, *16*, 1729 – 1736.
[45] J. L. Mergny, A. T. Phan, L. Lacroix, *FEBS Lett.* **1998**, *435*, 74 – 78.
[46] J. L. Mergny, L. Lacroix, *Oligonucleotides* **2003**, *13*, 515 – 537.

[47] R. D. Gray, J. B. Chaires, *Curr. Protoc. Nucleic Acid Chem.* **2011**, *45*, 17.4.1 – 17.4.16.
[48] P. Wallimann, R. J. Kennedy, J. S. Miller, W. Shalongo, D. S. Kemp, *J. Am. Chem. Soc.* **2003**, *125*, 1203 – 1220.
[49] R. Del Villar-Guerra, R. D. Gray, J. B. Chaires, *Curr. Protoc. Nucleic Acid Chem.* **2017**, *68*, 17.8.1 – 17.8.16.
[50] S. L. B. König, J. L. Huppert, R. K. O. Sigel, A. C. Evans, *Nucleic Acids Res.* **2013**, *41*, 7453 – 7461.
[51] J. L. Lippens, J. B. Mangrum, W. McIntyre, B. Redick, D. Fabris, *Rapid Commun. Mass Spectrom.* **2016**, *30*, 773 – 783.
[52] E. S. Baker, S. L. Bernstein, V. Gabelica, E. De Pauw, M. T. Bowers, *Int. J. Mass Spectrom.* **2006**, *253*, 225 – 237.
[53] A. C. Leney, A. J. R. Heck, *J. Am. Soc. Mass Spectrom.* **2017**, *28*, 5 – 13.
[54] T. Kenderdine, Z. Xia, E. R. Williams, D. Fabris, *Anal. Chem.* **2018**, *90*, 13541 – 13548.
[55] A. Marchand, V. Gabelica, *J. Am. Soc. Mass Spectrom.* **2014**, *25*, 1146 – 1154.
[56] M. Köhler, A. Marchand, N. B. Hentzen, J. Egli, A. I. Begley, H. Wennemers, R. Zenobi, *Chem. Sci.* **2019**, *10*, 9829 – 9835.
[57] A. Marchand, F. Rosu, R. Zenobi, V. Gabelica, *J. Am. Chem. Soc.* **2018**, *140*, 12553 – 12565.
[58] N. Jing, C. Marchand, J. Liu, R. Mitra, M. E. Hogan, Y. Pommier, *J. Biol. Chem.* **2000**, *275*, 21460 – 21467.
[59] N. Jing, X. Gao, R. F. Rando, M. E. Hogan, *J. Biomol. Struct. Dyn.* **1997**, *15*, 573 – 585.
[60] N. Smargiasso, F. Rosu, W. Hsia, P. Colson, E. S. Baker, M. T. Bowers, E. De Pauw, V. Gabelica, *J. Am. Chem. Soc.* **2008**, *130*, 10208 – 10216.
[61] G. Weber, *Adv. Protein Chem.* **1975**, *29*, 1 – 83.
[62] L. Petraccone, C. Spink, J. O. Trent, N. C. Garbett, C. S. Mekmaysy, C. Giancola, J. B. Chaires, *J. Am. Chem. Soc.* **2011**, *133*, 20951 – 20961.
[63] I. M. Pedroso, L. F. Duarte, G. Yanez, A. M. Baker, T. M. Fletcher, *Biochem. Biophys. Res. Commun.* **2007**, *358*, 298 – 303.
[64] F. M. Chen, *Biochemistry* **1992**, *31*, 3769 – 3776.
[65] H. Q. Yu, D. Miyoshi, N. Sugimoto, *J. Am. Chem. Soc.* **2006**, *128*, 15461 – 15468.
[66] "Quadruplex Nucleic Acids": L. Petraccone in *Topics in Current Chemistry*, *Vol. 330* (Eds.: J. Chaires, D. Graves), Springer, Berlin, **2012**, pp. 23 – 46.
[67] N. Q. Do, K. W. Lim, M. H. Teo, B. Heddi, A. T. Phan, *Nucleic Acids Res.* **2011**, *39*, 9448 – 9457.

Manuscript received: December 17, 2020
Revised manuscript received: March 7, 2021
Accepted manuscript online: April 6, 2021
Version of record online: May 26, 2021

